Regularized Progressive Expansion Algorithm for Recovery of Scattering Media from Time-Resolved Data

Wenwu Zhu and Yao Wang
Department of Electrical Engineering, Polytechnic University, Brooklyn, New York 11201

Harry L. Graber, Randall L. Barbour, and Jenghwa Chang
Departments of Pathology and Biophysics, State University of New York Health Science Center, Brooklyn, New York 11203

Abstract

A principal difficulty encountered in dealing with highly diffused signals is that the inverse problem is ill-posed and often underdetermined. A progressive expansion (PE) algorithm has previously been reported, which has proven to be quite effective in circumventing the underdetermined nature of the inverse problem. However, the PE approach is sensitive to noise. Propagation of errors can become especially severe when evaluating regions deep beneath the surface. Here we describe results of using a *Regularized PE* (RPE) algorithm, which is shown to exhibit improved stability. The RPE algorithm has been applied to time–resolved data calculated from a perturbation equation. The media tested include isotropically scattering slabs containing one or two compact absorbers at different depths below the surface. The data were corrupted by additive noise with varying strength. Compared to the original PE algorithm, the RPE algorithm has yielded more accurate and stable reconstructions under the same noise level.

Introduction

In this and accompanying reports, we consider the recovery of scattering media having optical properties similar to tissue, based on either experimental continuous wave (CW) or simulated time–resolved (TR) near infrared optical measurements. The problem is difficult because in this frequency range photons propagate through the tissue in a highly diffused manner and the relation between the measured signal and the absorption properties of the media is non-linear. In the past few years, our group has developed an iterative perturbation approach for both CW and TR data [1-3]. This requires the solution of a linear perturbation equation at each iteration:

$$\mathbf{W}\Delta\mathbf{x} = \Delta\mathbf{I}, \tag{1}$$

where $\Delta\mathbf{x}$ is a vector of differences in the absorption properties between a reference and test medium, $\Delta\mathbf{I}$ a vector of changes in detector readings between the two media, and $\mathbf{W}$ a matrix of weights describing the influence of each volume element (voxel) on the detector readings, which are essentially the derivatives of the detector readings with respect to the absorption coefficients in the reference medium. In practice, the perturbation equation is in general both underdetermined and ill-conditioned. The underdeterminedness results from the number of detector readings, M, being less than the number of unknowns N. Even if $M \geq N$, the matrix $\mathbf{W}$ can be rank deficient, which also leads to an underdetermined system. The cause of the ill–conditioning is that $\mathbf{W}$ contains many nearly zero columns. Very small variations in $\Delta\mathbf{I}$ can result in very large deviations in $\Delta\mathbf{x}$.

Our previous studies have focused on how to overcome the underdeterminedness problem. We have developed a multigrid method for CW data [1] and a progressive expansion (PE) algorithm for TR data [2]. The PE algorithm evaluates increasing depths within the medium by successively considering signals entering the detector at increasing times following an incident pulse. Instead of solving Eq. (1) directly, a subsystem represented by

$$\mathbf{W}_l\Delta\mathbf{x}_l = \Delta\mathbf{I}_l \tag{2}$$

is solved at each time interval l. Here, $\Delta\mathbf{x}_l$ consists of the voxels which can contribute signals at

OSA Proceedings on Advances in Optical Imaging and Photon Migration, 1994, Vol. 21, R. R. Alfano (ed.)

this time interval but not earlier, $\Delta \mathbf{I}_l$ includes detector readings after subtracting the contributions from the previously determined voxels, and $\mathbf{W}_l$ consists of the weights with respect to the elements in $\Delta \mathbf{x}_l$ only. As long as the very early signals can be detected, the subsystem at each time interval will be determined or overdetermined. In this case, $\mathbf{W}_l^T \mathbf{W}_l$ is invertible, and there exists a unique least squares (LS) solution for each subsystem:

$$\Delta \mathbf{x}_l = (\mathbf{W}_l^T \mathbf{W}_l)^{-1} \mathbf{W}_l^T \Delta \mathbf{I}_l, \tag{3}$$

which minimizes the following error:

$$E(\Delta \mathbf{x}_l) = \| \mathbf{W}_l \Delta \mathbf{x}_l - \Delta \mathbf{I}_l \|^2 . \tag{4}$$

This technique is very effective in circumventing the underdetermined nature of the inverse problem. However, because of the ill–conditioning of $\mathbf{W}_l$, the LS solution at each time interval is sensitive to noise. The error in shallower regions which are solved using earlier data can also propagate into deeper regions. This error propagation effect can become especially severe when the algorithm probes deep beneath the surface. In order to overcome this problem, an overlapping scheme has been developed. With this method, the absorption in a voxel is not fixed the first time it is computed. Rather, it is reconsidered in the next several time intervals. This mechanism can greatly reduce the error propagation and provide more reliable reconstruction.

In order to further improve the stability of the PE algorithm, we have incorporated the Tikhonov–Miller regularization method [4,5] in the solution of the subsystem at each time gate. The RPE algorithm and experimental results with both PE and RPE algorithms are presented below. For convenience, we omit the subscript l in the following discussion.

The Regularized Progressive Expansion Algorithm

Regularization is a well-established technique for dealing with instability in inverse problems and can convert an ill-posed problem into a well-posed problem by incorporating *a priori* knowledge about the image to be recovered. Using the Tikhonov-Miller regularization approach, the idea is to choose an approximate solution from a set of admissible solutions using a defined criterion. The class of feasible solutions is defined as: $S_{\mathbf{\Delta x}/\mathbf{\Delta I}}(\mathbf{\Delta x}) = \{\mathbf{\Delta x} : \| \mathbf{W\Delta x} - \mathbf{\Delta I} \|^2 \leq \epsilon^2\}$. The bound ϵ^2 depends on the noise level of the observed data. Tikhonov defined the regularized solution to be the one which minimizes a stable functional $\| \mathbf{C\Delta x} \|^2$ subject to the constraint $\| \mathbf{W\Delta x} - \mathbf{\Delta I} \|^2 = \epsilon^2$. Here, $\mathbf{C}$ is a *regularization operator* and can be selected according to *a priori* knowledge. If the solution is known to be bounded but fluctuating, we can take $\mathbf{C}$ to be an identity matrix. If the solution is continuous, then we can take $\mathbf{C}$ as the first-order differential operator. If we know the solution is smooth, then $\mathbf{C}$ can be chosen to be a second-order differential operator. Then, using the Lagrange multipliers method, the problem is to minimize:

$$E(\mathbf{\Delta x}) = \|\mathbf{W\Delta x} - \mathbf{\Delta I}\|^2 + \lambda \|\mathbf{C\Delta x}\|^2, \tag{5}$$

where the *regularization parameter* λ can be solved from the previously described constraint. The regularized solution is given by

$$\mathbf{\Delta x} = (\mathbf{W}^T\mathbf{W} + \lambda \mathbf{C}^T\mathbf{C})^{-1}\mathbf{W}^T\mathbf{\Delta I}. \tag{6}$$

Miller took a set theoretic approach and constrained the solution on both $S_{\mathbf{\Delta x}/\mathbf{\Delta I}}$ and the set $S_{\mathbf{\Delta x}}(\mathbf{\Delta x}) = \{\Delta x : \| \mathbf{C\Delta x} \|^2 \leq E^2\}$, where E is a constant. The two constraints can be combined into a quadratic formula. The solution is identical to Tikhonov regularization with $\lambda = \epsilon^2/E^2$, the so-called Miller criterion. Numerically, we can see that the solution of Eq. (6) is more stable than that of Eq. (3), because $\mathbf{W}^T\mathbf{W} + \lambda \mathbf{C}^T\mathbf{C}$ is better conditioned than $\mathbf{W}^T\mathbf{W}$.

Since the dimension of $\mathbf{W}$ can be extremely large, we do not perform matrix inversion directly to obtain the solutions in Eqs. (3) and (6). Rather, we minimize the functional in Eq. (6) using the conjugate gradient descent (CGD) method. The n-th iteration of the CGD algorithm can be described by:

$$\mathbf{g}^{(n)} = \mathbf{W}^T(\mathbf{W\Delta x}^{(n)} - \mathbf{\Delta I}) + \lambda \mathbf{C}^T\mathbf{C\Delta x}^{(n)},$$
$$\mathbf{d}^{(n)} = \mathbf{g}^{(n)} + (\| \mathbf{g}^{(n)} \|^2 / \| \mathbf{g}^{(n-1)} \|^2)\mathbf{d}^{(n-1)},$$
$$\alpha^{(n)} = (\mathbf{d}^{(n)}, \mathbf{g}^{(n)}) / (\| \mathbf{Wd}^{(n)} \|^2 + \lambda \| \mathbf{Cd}^{(n)} \|^2),$$
$$\mathbf{\Delta x}^{(n+1)} = \mathbf{\Delta x}^{(n)} + \alpha^{(n)}\mathbf{d}^{(n)}.$$

In our current implementation, the regularization operator $\mathbf{C}$ is chosen to be an identity to make use of the bounded nature of the solution. We further assume that the upper bounds on $\|\mathbf{W\Delta x} - \mathbf{\Delta I}\|^2$ and $\|\mathbf{Cx}\|^2$ can be estimated from measurement data or prior knowledge, and determine the regularization parameter λ by the Miller criterion.

Experimental Results

In this section, we compare the reconstruction results obtained by PE and RPE for several test media

containing compact absorbers. In the following experiments, the source configuration and detector distribution are the same as in [2]. Only one iteration of the perturbation method has been performed, using the medium without absorbers as the reference. The weights for this medium were calculated using Monte Carlo simulations [6]. Values for $\mathbf{\Delta I}$ were first calculated based on Eq.(1). Gaussian noise was then added to evaluate the algorithm's sensitivity to noise. The ratio of the noise deviation to the mean value of the difference in detector readings is used as the measure of the noise level.

In the first experiment, two closely juxtaposed absorbers of size 1 cubic mean free path (mfp; 1 mfp = the average distance a photon propagates between successive interactions with the medium), separated by 1 mfp, were buried between 4 mfp and 5 mfp in a 10 mfp thick slab [6]. In the second experiment, one single absorber of size 8 cubic mfp was buried between 10 mfp and 12 mfp in a 20 mfp thick slab. In the third experiment, two absorbers, one directly above the other, were buried at depth 2-4 mfp and 6-8 mfp in a 20 mfp thick slab. In the fourth experiment, one absorber of size 8 cubic mfp was buried at depth 6-8 mfp in the center, and three contiguous absorbers of the same size were buried at depth 10-12 mfp in a 20 mfp thick slab. In all experiments, 10% noise was added in the detector readings. In each experiment, the regularization parameter λ was chosen according to Miller criterion, since we usually know the bound of the reconstructed image and noise variance in the detector readings. The regularization operator $\mathbf{C}$ was chosen to be an indentity matrix. An overlapping interval of 3 mean free time (mft; 1 mft = 1 mfp/c, where c is the speed of light in the medium) is used in both PE and RPE algorithms.

The reconstructed results from these experiments are illustrated in Figs. 1 to 4. Figs. 1, 2 and 4(a) are the original images, Figs. 1, 2 and 4(b) are the reconstructed images using the PE algorithm at time 17 mft, 26 mft and 24 mft, respectively. Figs. 1, 2 and 4(c) are the reconstructed images using the RPE algorithm at the same times as in (b). In order to explain the stability of RPE and to show how effective it is at suppressing noise, we show the reconstructed images at different time windows in Fig. 3. Fig. 3(a) is the original image, (b) and (c) are the reconstructed images using PE at time 22 mft and 28 mft, respectively; (e) and (f) are the reconstructed images using RPE at time 22 mft and 28 mft, respectively. In all figures, the left column is the X-Z cross-section of the medium and the right column is the Y-Z cross-section. For display purposes, the reconstructed values are quantized into 10 levels. Further, the images have been scaled individually so that the maximum intensity value in each image is represented by the same darkness. Therefore, the same level in different figures may represent different absorption levels, especially in the reconstructed images without regularization, in which the maximum values are usually much greater than that in the reconstructed images with regularization. In fact, the maximum value obtained without regularization usually reaches the preset upper bound, greatly exceeding the real value in the test medium. From these results, we can see that the PE algorithm converged to a solution containing numerical artifacts comparable in magnitude to the target. The RPE algorithm, on the other hand, yielded a solution much more closely resembling the original medium. In fact, the PE algorithm tends to diverge after a certain time interval because of strong error propagation in the presence of noise, as shown in Fig. 3 (c), while the RPE algorithm can successfully suppress this effect for noise levels up to 10%.

In terms of computation time, when both the PE and RPE algorithms are run on a parallel computer (Kilonode [7]), the computation time of the RPE algorithm is increased by about 10% over the PE algorithm.

Conclusion and Discussion

In this study, Tikhonov–Miller regularization has been incorporated into the PE algorithm previously proposed for image reconstruction from TR data. Our experimental results have shown that it is very effective in stablizing the PE algorithm and suppressing error propagation. Arridge *et al.* have reported the use of a Tikhonov regularization algorithm and the Levenberg–Marquardt algorithm for image reconstruction from CW and mean–time–of–flight data [8, and references therein]. We have considered a much larger 3D problem rather than a 2D problem, at a higher noise level, and the reconstruction was based on a much more restricted data set (back-scattered signal in response to a single source only).

A critical problem in the use of regularization is the selection of the parameter λ when the upper bounds on $||\mathbf{W\Delta x} - \mathbf{\Delta I}||^2$ and/or $||\mathbf{C\Delta x}||^2$ are unknown. If only one of the bounds is known, a *constrained least–squares* approach can be followed [9]. When both bounds are unavailable, the *cross-validation* method [10] can be used. One disadvantage of these two approaches is that they require

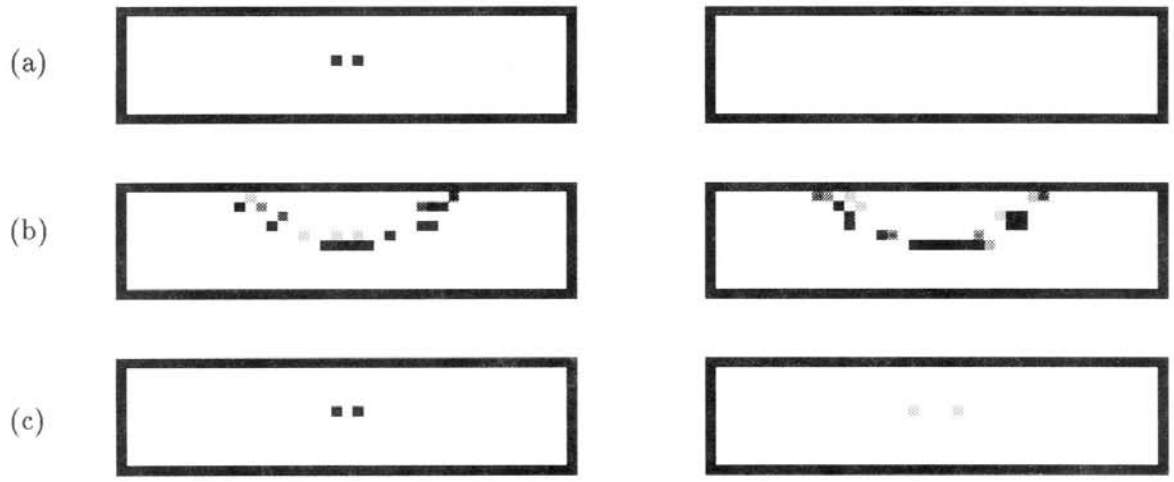

Figure 1: Reconstruction of a 10 mfp (mean free path) thick slab medium containing two 1 cubic mfp absorbers, separated by 1 mfp, at depth 4-5 mfp. Left column: X-Z cross-section, right column: Y-Z cross-section. Within each column: (a) original medium, (b) reconstruction by PE with an overlapping interval of 3 mft (mean free time); and (c) reconstruction by RPE with the same overlapping interval. The noise level was 10%. All the reconstructed images are obtained after 17 time windows of width 1 mft. The maximum values level in (a), (b) and (c) correspond to 0.01,0.1 and 0.0091 respectively.

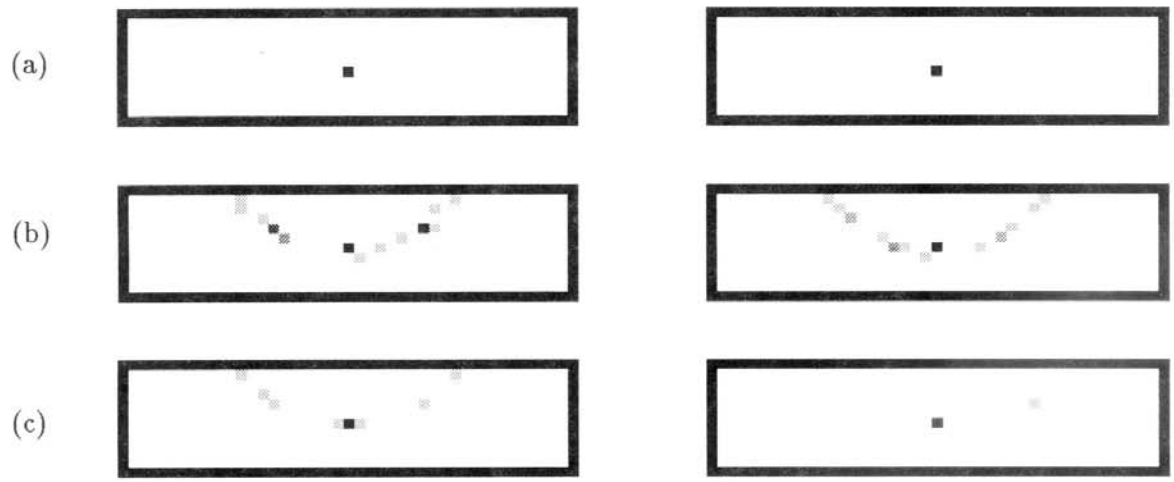

Figure 2: Reconstruction of a 20 mfp thick slab medium containing one absorber of size 8 cubic mfp at depth 10-12 mfp. Left column: X-Z cross-section, right column: Y-Z cross-section. Within each column: (a) original medium, (b) reconstruction by PE with an overlapping interval of 3 mft; and (c) reconstruction by RPE with the same overlapping interval. The noise level was 10%. All the reconstructed images are obtained after 26 time windows of width 2 mft. The maximum values level in (a), (b) and (c) correspond to 0.01,0.1 and 0.01 respectively.

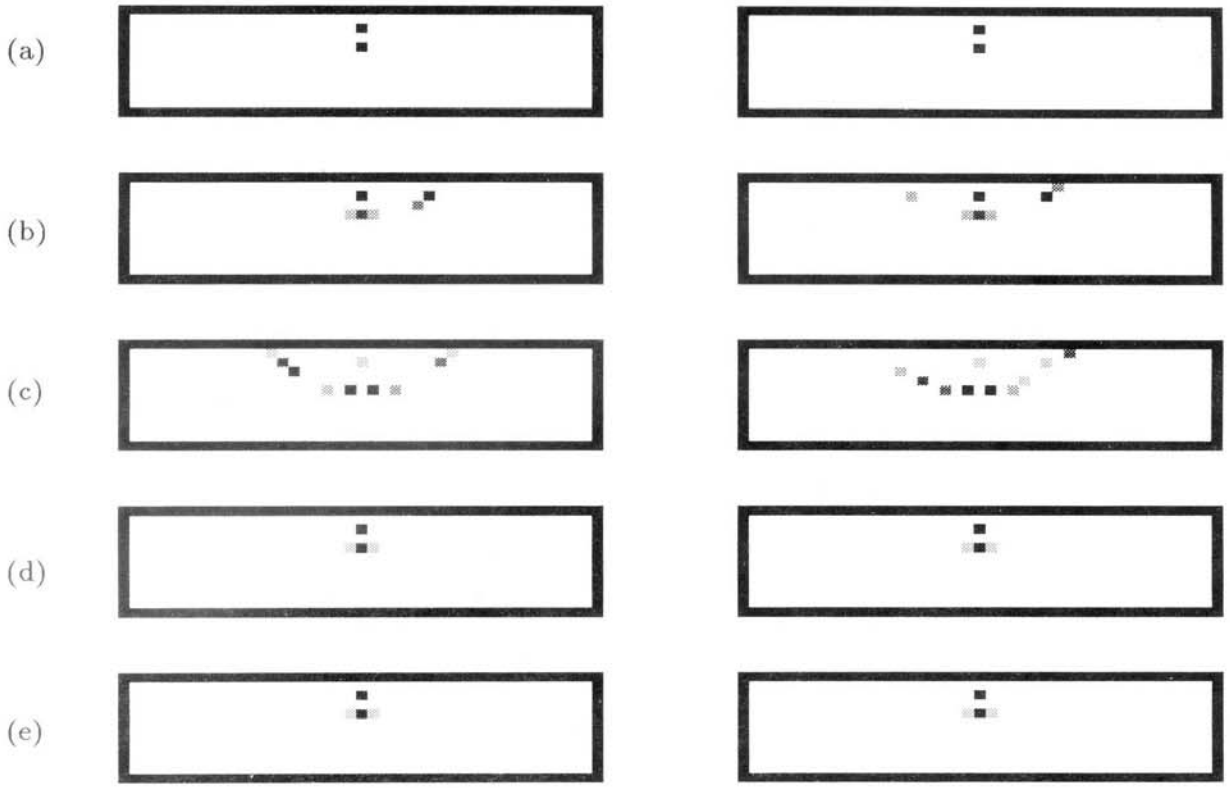

Figure 3: Reconstruction of a 20 mfp thick slab medium containing two 8 cubic mfp absorbers, one above the other, at depth 2-4 mfp and depth 6-8 mfp. (a) original medium, (b) and (c) reconstruction by PE with an overlapping interval of 3 mft after 22 time windows and 28 time windows of width 2 mft, respectively; (e) and (f) reconstruction by RPE with the same overlapping interval after 22 time windows and 28 time windows of width 2 mft, respectively. The noise level was 10%. The maximum values level in (a), (b), (c), (d) and (e) correspond to 0.01, 0.01, 0.1, 001 and 0.01 respectively.

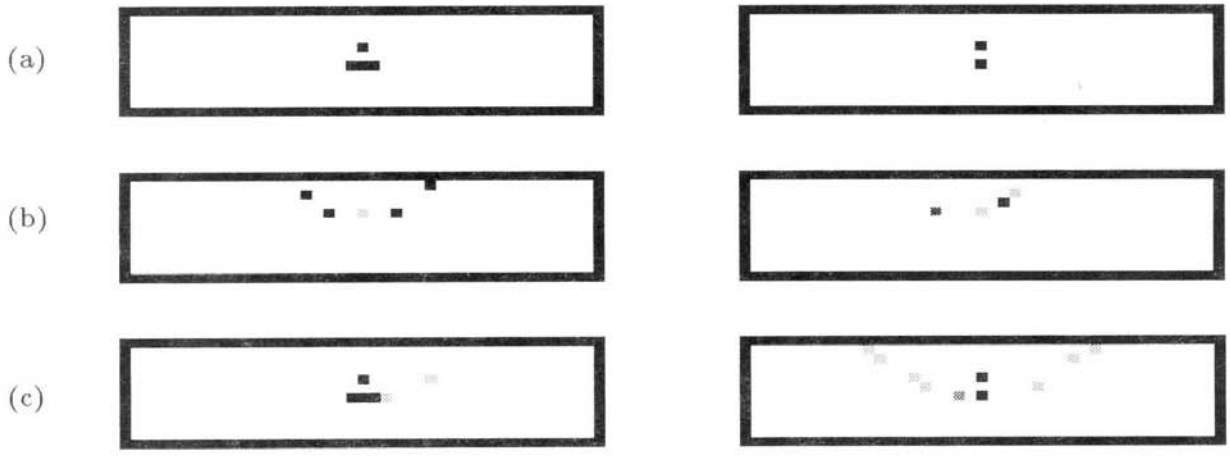

Figure 4: Reconstruction of a 20 mfp thick slab medium containing one absorber of size 8 cubic mfp at depth 6-8 mfp and three contiguous absorbers of the same size at depth 10-12 mfp. (a) original medium, (b) reconstruction by PE with an overlapping interval of 3 mft; and (c) reconstruction by RPE with the same overlapping interval. The noise level was 10%. All the reconstructed images are obtained after 24 time windows of width 2 mft. The maximum values level in (a), (b) and (c) correspond to 0.01,0.1 and 0.01 respectively.

an overwhelming amount of computation when the weight matrix is large. When incorporating regularization in our PE algorithm, this computation would have to be repeated for each time-window. Recently, an algorithm has been developed by Kang and Katsaggelos [11] that obtains the regularized least squares solution iteratively using a gradient descent method, and at each iteration calculates an updated regularization parameter λ based on the previous solution. The algorithm is powerful, in that λ upon convergence does not depend on the initial estimate of $\mathbf{\Delta x}$. Because λ does not need to be determined in a separate initial step, additional computational overhead is minimal. The incorporation of this approach in RPE will be investigated in future studies. Another problem to be investigated is what kind of regularization operator, $\mathbf{C}$, is appropriate for our problem. Studies can be performed that compare the results obtained by using the 0-th, 1-st, and 2-nd order derivatives of the image $\mathbf{\Delta x}$.

References

[1] Y. Wang, J. Chang, R. Aronson, R.L. Barbour, H.L. Graber, and J. Lubowsky, "Imaging scattering media by diffusion tomography: An iterative perturbation approach," in *Proc. Physiological Monitoring and Early Detection Diagnostic Methods*, vol. SPIE-1641, (Los Angeles), pp. 58–71, Jan. 1992.

[2] J. Chang, Y. Wang, R. Aronson, H. L. Graber, and R.L. Barbour, "A layer-stripping approach for recovery of scattering media from time-resolved data," in *Proc. Inverse Problems in Scattering and Imaging*, vol. SPIE–1767, (San Diego), pp. 384–395, July 1992.

[3] R. L. Barbour, H. L. Graber, Y. Wang, J. Chang, and R. Aronson, "A perturbation approach for optical diffusion tomography using continuous-wave and time-resolved data," *SPIE Medical Optical Tomography — Functional Imaging and Monitoring*, SPIE Institutes, IS11, pp. 87-120, 1993.

[4] A. N. Tikhonov and V. Y. Arsenin, *Solution of Ill-Posed Problems*, Washington D. C.: V. H. Winston, 1977.

[5] K. Miller, "Least squares method for ill–posed problems with a prescribed bound," *SIAM J. of Mathematical Analysis*, vol. 1, pp. 52–74, Feb. 1970.

[6] H. L. Graber, J. Chang, R. Aronson and R. L. Barbour, "A perturbation model for imaging in dense scattering media: derivation and evaluation of imaging operators," *Medical Optical Tomography — Functional Imaging and Monitoring*, SPIE Institutes, IS11, pp.121-43, 1993.

[7] F. H. Schlereth, J. M. Fossaceca, A. D. Keckler and R. L. Barbour, "Imaging of diffusing media with a neural net formulation: A problem in large scale computation," in *Proc. Physiological Monitoring and Early Detection Diagnostic Methods*, vol. SPIE-1641, (Los Angeles), pp. 46–57, Jan. 1992.

[8] S. R. Arridge, "The forward and inverse problems in time resolved infra-red imaging," *SPIE Medical Optical Tomography — Functional Imaging and Monitoring*, SPIE Institutes, IS11, pp. 35-64, 1993.

[9] B. R. Hunt, "Application of constrained least squares estimation to image restoration by digital computers," *IEEE Trans. Comput.*, vol. C-22,pp. 805–812, 1973.

[10] G. H. Golub, M. Heath, and G. Wahba, "Generalized cross-validation as a method for choosing a good ridge parameter," Technometrics, vol. 21, No. 2, pp. 215-223, 1979.

[11] M. G. Kang and A. K. Katsaggelos, "Regularized iterative image restoration based on an iterative updated convex smoothing functional," *Proc. SPIE Visual Communications and Image Processing Conf.*, vol. SPIE-2094, (Cambridge), pp. 1364–1372, Nov. 1993.

Acknowledgement

This work was supported in part by the National Institutes of Health under Grant # RO1-CA59955 and by the New York State Science and Technology Foundation.